ISSN 1674-1056
http://cpb.iphy.ac.cn
http://iopscience.iop.org/cpb
中国物理 B
Chinese Physics
中国物理 Chinese Physics B

High birefringence, low loss, and flattened dispersion photonic crystal fiber for terahertz application

Dou-Dou Wang(王豆豆), Chang-Long Mu(穆长龙), De-Peng Kong(孔德鹏), Chen-Yu Guo(郭晨瑜)
Citation: Chin. Phys. B . 2019, 28(11): 118701 . **doi:** 10.1088/1674-1056/ab44af
Journal homepage: http://cpb.iphy.ac.cn; http://iopscience.iop.org/cpb

What follows is a list of articles you may be interested in

Terahertz coherent detection via two-color laser pulses of various frequency ratios

Xin-Yang Gu(顾新杨), Ke-Jia Wang(王可嘉), Zhen-Gang Yang(杨振刚), Jin-Song Liu(刘劲松)
Chin. Phys. B . 2019, 28(9): 098701 . **doi:** 10.1088/1674-1056/ab37fc

Effect of terahertz pulse on gene expression in human eye cells

Jin-Wu Zhao(赵晋武), Ming-Xia He(何明霞), Li-Jie Dong(东莉洁), Shao-Xian Li(李绍限), Li-Yuan Liu(刘立媛), Shao-Chong Bu(步绍翀), Chun-Mei Ouyang(欧阳春梅), Peng-Fei Wang(王鹏驰), Long-Ling Sun(孙珑玲)
Chin. Phys. B . 2019, 28(4): 048703 . **doi:** 10.1088/1674-1056/28/4/048703

Theoretical investigation of tunable polarized broadband terahertz radiation from magnetized gas plasma

Xin-Yang Gu(顾新杨), Jin-Song Liu(刘劲松), Zhen-Gang Yang(杨振刚), Sheng-Lie Wang(汪盛烈), Ke-Jia Wang(王可嘉)
Chin. Phys. B . 2018, 27(5): 058701 . **doi:** 10.1088/1674-1056/27/5/058701

Ultra-compact terahertz switch with graphene ring resonators

Jian-Zhong Sun(孙建忠), Le Zhang(章乐), Fei Gao(高飞)
Chin. Phys. B . 2016, 25(10): 108701 . **doi:** 10.1088/1674-1056/25/10/108701

Performance analysis of LDPC codes on OOK terahertz wireless channels

Chun Liu(刘纯), Chang Wang(王长), Jun-Cheng Cao(曹俊诚)
Chin. Phys. B . 2016, 25(2): 028702 . **doi:** 10.1088/1674-1056/25/2/028702

High birefringence, low loss, and flattened dispersion photonic crystal fiber for terahertz application*

Dou-Dou Wang(王豆豆)[1,†], Chang-Long Mu(穆长龙)[1], De-Peng Kong(孔德鹏)[2], and Chen-Yu Guo(郭晨瑜)[1]

[1] College of Sciences, Xi'an University of Science and Technology, Xi'an 710054, China
[2] The State Key Laboratory of Transient Optics and Photonics, Xi'an Institute of Optics and Precision Mechanics, Chinese Academy of Sciences, Xi'an 710119, China

(Received 26 June 2019; revised manuscript received 14 August 2019; published online 16 October 2019)

A type of photonic crystal fiber based on Kagome lattice cladding and slot air holes in a rectangular core is investigated. Full vector finite element method is used to evaluate the modal and propagation properties of the designed fiber. High birefringence of 0.089 and low effective material loss of 0.055 cm^{-1} are obtained at 1 THz. The *y*-polarized fundamental mode of the designed fiber shows a flattened and near-zero dispersion of 0 ± 0.45 $ps\cdot THz^{-1}\cdot cm^{-1}$ within a broad frequency range (0.5 THz–1.5 THz). Our results provide the theory basis for applications of the designed fiber in terahertz polarization maintaining systems.

Keywords: terahertz, photonic crystal fiber, birefringence, loss, dispersion

PACS: 87.50.U–, 42.81.Qb, 42.81.Gs **DOI:** 10.1088/1674-1056/ab44af

1. Introduction

The electromagnetic wave located between the microwaves and infrared region is commonly defined as terahertz (THz) radiation with frequency domain from 0.1 THz to 10 THz. Recently, terahertz radiation has attracted significant attention due to its potential applications in sensing,[1] imaging,[2] time-domain spectroscopy,[3] pharmaceutical drug testing,[4] and communication,[5] *etc*. However, THz systems that rely on free-space and bulk optics to transport and manipulate the THz radiation are large and immobile, difficult to use and integrate with infrared and optical systems. In order to solve this problem, various THz waveguides have been reported, including metallic waveguides,[6] dielectric tubes,[7] Bragg fibers,[8] plastic ribbons,[9] photonic crystal fibers (PCFs),[10–17] *etc*. Porous core PCFs have aroused the interest of the researchers widely for their low absorption loss, low dispersion, and high degree of design freedom. Besides, high birefringence can be achieved by breaking the symmetry of the core or cladding region of the porous core PCFs.

THz fiber with high birefringence has potential applications in THz systems, so a variety of highly birefringent THz PCFs have been investigated in recent years. Cho *et al.*[11] fabricated a plastic PCF that exhibits a birefringence of 0.021 at 0.3 THz. Atakaramians *et al.*[12] designed a porous fiber with slot air holes and obtained a birefringence of about 0.026 at 0.6 THz. Chen *et al.*[13] proposed a porous fiber with elliptical air-holes and obtained a high birefringence of 0.047 at 1.22 THz with the elliptical air-holes rotating at 30°. Hasan *et al.*[14] designed a spiral PCF with artificial asymmetry in the porous core and obtained a birefringence of 0.0483 at 1 THz.

Low loss and other characteristics, such as flattened and near-zero dispersion are necessary for practical applications of THz fibers, in addition to high birefringence. Wu *et al.*[15] proposed an oligoporous-core THz PCF with a birefringence of 0.03 and a low effective material loss of about 20%–40% of its bulk material loss. Habib *et al.*[16] presented a THz fiber with a rectangular core to realize a birefringence of 0.018 at 1 THz and a low flattened dispersion of 1.1 ± 0.02 $ps\cdot THz^{-1}\cdot cm^{-1}$ in a frequency range of 0.8 THz–1.2 THz. Islam *et al.*[17] designed an oligoporous-core PCF with Kagome lattice cladding, which has a high birefringence of 0.079, low effective material loss of 0.05 cm^{-1} at 1 THz. Although the performances (*i.e*., the low loss, high birefringence, low/flattened dispersion) of THz PCFs have been improved individually or wholly, there is still much room for further improvement by designing fiber structures.

In this paper, a THz PCF with Kagome-structured cladding and rectangular core with slot air holes is designed. The designed PCF presents high birefringence, low loss and flattened near zero dispersion properties in a broad frequency range. The designed fiber structure has not been reported to the best of our knowledge, and it has potential applications in polarization-maintaining THz systems.

2. Fiber structure design

Cross section of the designed THz PCF is shown in Fig. 1. The Kagome-structured cladding (with lattice pitch

*Project supported by the National Natural Science Foundation of China (Grant No. 11604260) and the Outstanding Youth Science Fund of Xi'an University of Science and Technology, China (Grant No. 2019YQ3-10).

†Corresponding author. E-mail: wangdoudou@xust.edu.cn

© 2019 Chinese Physical Society and IOP Publishing Ltd

Λ and Topas strut thickness t) is adopted as its compact design and extremely low confinement loss in a broad frequency range.[17] A rectangular core with five slot air holes is designed to induce the high birefringence and reduce the material absorption loss. L and W ($L = 3\Lambda/2$, $W = \sqrt{3}\Lambda/2$) donate the length and width of the rectangular core, respectively. The slot core air holes with equal intervals (center-to-center distance between two adjacent slot-core-holes is $W/5$) and different widths (h and $3h$) are designed to improve birefringence and reduce material absorption loss.

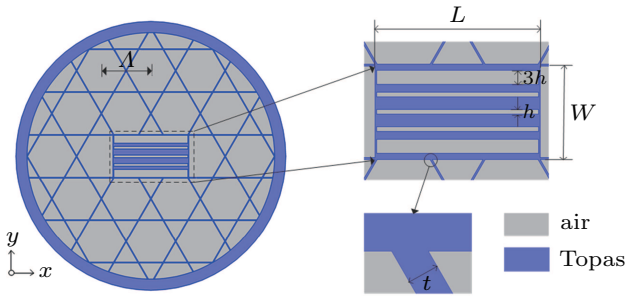


Fig. 1. Cross section of designed PCF.

Material Topas is used as a background material in our design on account of its low material dispersion (with a constant refractive index of 1.5258) and relatively low material loss (rises at a rate of 0.36 cm^{-1}/THz from 0.06 cm^{-1} at 0.4 THz) in a range of 0.1 THz–1.5 THz,[18] low water absorption ($\sim 1/10$ of the PMMA), and chemical resistance to common solvents.[19]

3. Results and discussion

The modal and propagation properties of the designed THz PCF are studied theoretically with the finite element method (FEM). Perfectly matched layer (PML) absorbing boundary condition is used to calculate the confinement loss.

As an important parameter for a polarization maintaining THz waveguide, the birefringence is defined as the absolute difference between the effective indexes of x- and y-polarized fundamental modes:[13]

$$B = \left| n_{\text{eff}}^{x} - n_{\text{eff}}^{y} \right|, \tag{1}$$

where n_{eff}^{x} and n_{eff}^{y} are the real part of the effective refractive index for x- and y-polarized fundamental modes, respectively. From the definition point of view, birefringence can be increased by maximizing the difference between the mode field distributions of the x- and y-polarized fundamental modes.

The major transmission loss of PCF can be attributed to material absorption loss and confinement loss (CL). It is hard to fabricate a low loss THz fiber experimentally due to the fact that all materials except dry air have relatively high absorption coefficient for THz radiation. The material absorption loss of THz fiber can be reduced by maximizing the power fraction of the fundamental modes in air. The effective material loss (EML) of the fundamental modes, caused by material absorption, can be expressed as[20]

$$\alpha_{\text{eff}} = \sqrt{\frac{\varepsilon_0}{\mu_0}} \left(\frac{\int_{\text{mat}} n_{\text{mat}} |\boldsymbol{E}|^2 \alpha_{\text{mat}} \, \mathrm{d}A}{2 \left| \int_{\text{all}} S_z \, \mathrm{d}A \right|} \right), \tag{2}$$

where ε_0 and μ_0 are the permittivity and permeability of the vacuum, respectively, n_{mat} and α_{mat} are the refractive index and bulk material absorption loss of Topas, respectively, $\boldsymbol{E}$ is the electric field component, S_z is the z-component of the Poynting vector.

The CL depends mainly on the number of cladding hole rings and core porosity, it represents the ability to restrict the light in the core. The CL can be calculated from the following expression[21]

$$\alpha_{\text{CL}} = 8.686 \times \left(\frac{2\pi f}{c} \right) \text{Im}(n_{\text{eff}}), \tag{3}$$

in decibels per meter, where $\text{Im}(n_{\text{eff}})$ is the imaginary of the complex effective refractive index, f is the operating frequency, and c is the speed of light in vacuum.

Dispersion is also an important propagation property for THz waveguide as it degrades the signal in broadband or long distance transmission. Flattened and near-zero dispersion is necessary for the effective transmission of broadband THz waves. Firstly, it is necessary to ensure single mode propagation in order to reduce intermodal dispersion. The single mode condition for index guiding PCF can be determined by the normalized frequency expressed by the V-parameter[13]

$$V = \frac{2\pi r f}{c} \sqrt{n_{\text{co}}^2 - n_{\text{cl}}^2} \leq 2.405, \tag{4}$$

where r is the radius of the fiber core (regarded as $L/2$ and $W/2$ for the x- and y-polarized fundamental modes, respectively), n_{co} and n_{cl} are the effective refractive indexes of the core and cladding, respectively. We evaluate the single mode condition with $n_{\text{co}} = n_{\text{eff}}$, and n_{cl} is taken as 1 due to the high air fraction of the cladding for the designed PCF. When the fiber operates in single mode condition, the dispersion can be attributed to material dispersion and waveguide dispersion. Material dispersion of the designed fiber can be neglected due to the fact that the background material Topas has a constant refractive index in a range of 0.1 THz–1.5 THz, so the dispersion is mainly caused by waveguide dispersion. In the THz region, group-velocity dispersion (GVD) can be calculated from the following equation[21]

$$\beta_2 = \frac{2}{c} \frac{\mathrm{d}n_{\text{eff}}}{\mathrm{d}\omega} + \frac{\omega}{c} \frac{\mathrm{d}^2 n_{\text{eff}}}{\mathrm{d}\omega^2}, \tag{5}$$

where $\omega = 2\pi f$.

Different core structures have been studied in order to obtain high birefringence. We find that the core structure with different slot air hole widths (defined as core 1) can introduce higher birefringence than the one with equal slot air hole width (defined as core 2) although their porosities are equal as shown in Fig. 2. Therefore, core 1 is adopted in the following study.

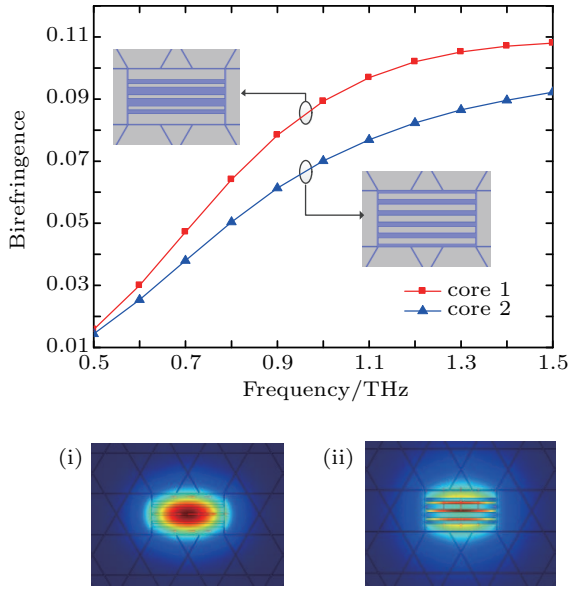


Fig. 2. Plots of birefringence *versus* frequency for two different core structures and mode profiles of the (i) x- and (ii) y-polarized fundamental modes at 1 THz ($\Lambda = 200$ μm, $t = 0.015\Lambda$, core porosity = 55%).

Figures 2(i) and 2(ii) are the mode profiles (power flow) of the x- and y-polarized fundamental modes for the designed PCF at 1 THz, respectively. It can be found that both the x- and y-polarized fundamental modes are well confined in the core region, but the former has better confinement (lower CL) and the latter has higher power fraction distributed in the slot core air hole (lower EML). The large difference between the x- and y-polarized fundamental mode profiles is due to the breaking of six-fold symmetry in the core.

Scalability dependence of the birefringence and EML have been studied in order to obtain the optimal structure parameters. Figure 3 shows the variation of birefringence and EML with respect to lattice pitch. It can be found that EML for both the x-polarized (x-pol) and y-polarized (y-pol) fundamental modes increases with lattice pitch increasing. This can be explained by the fact that larger lattice pitch means larger core and electromagnetic waves interact greatly with the material Topas, thus the EML increases. What is more, the EML of y-polarized fundamental mode is lower than that of the x-polarized fundamental mode, which is inconsistent with the mode field distribution as shown in Fig. 2. However, birefringence has a maximum value when the lattice pitch is 300 μm, which equals the guided wavelength. Considering a tradeoff between high birefringence and low EML, the value of Λ is fixed at 200 μm for the following study.

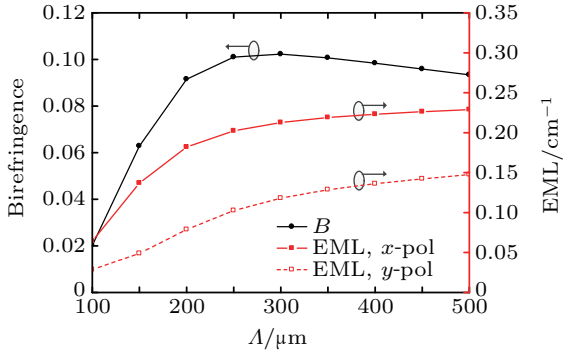


Fig. 3. Birefringence and EML *versus* lattice pitch at 1 THz ($t = 0.015\Lambda$, core porosity = 55%).

For realistic PCFs, the guided modes are inherently leaky as a result of the finite number of cladding hole rings, and confinement loss occurs inevitably. However, transmission loss of THz PCF is mainly derived from material absorption loss rather than confinement loss, especially for the PCF with Kagome lattice cladding. In order to make it flexible and compact, the THz fiber should be as thin as possible, *i.e.*, the cladding hole rings should be as few as possible. Figure 4 shows the variation of birefringence, EML and CL with cladding hole ring number. It can be found that birefringence and EML have little change, although CL decreases dramatically with the cladding hole ring number increasing. Even two rings of cladding holes can obtain a negligible CL compared with the EML. So two rings of cladding hole structure are both adopted for the designed fiber.

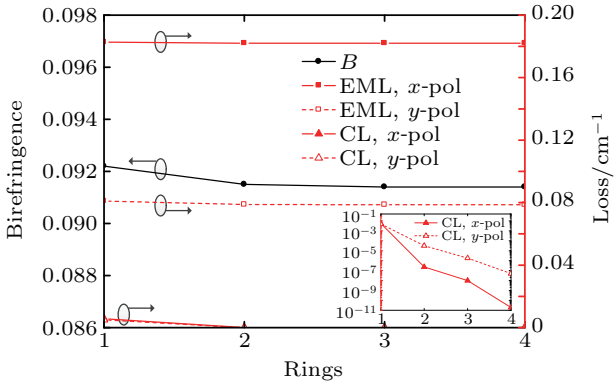


Fig. 4. Birefringence and loss (EML and CL) *versus* cladding hole ring number at 1 THz, with inset showing magnified variation trend of CL ($\Lambda = 200$ μm, $t = 0.015\Lambda$, core porosity = 55%).

For an index guiding porous-core PCF, the material absorption loss can be reduced by maximizing the power fraction of the fundamental modes in air, which is closely related to the core porosity. Figure 5 shows the variation of birefringence and EML with core porosity in a range from 20% to 55% which is the maximum value for the designed core structure. It can be seen that the EML decreases linearly with the core porosity increasing. The variation of birefringence with core porosity is relatively small although it has a maximum value

when the core porosity is around 40%. So the core porosity of 55% is adopted as an optimal structural parameter due to its low EML.

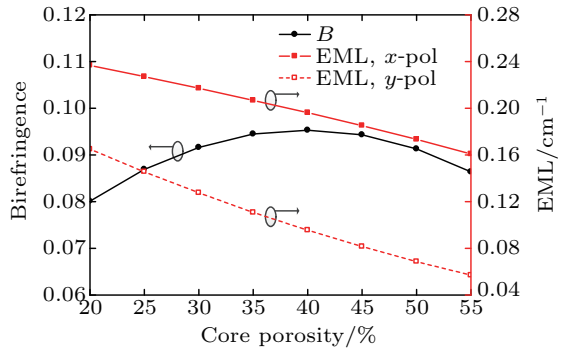


Fig. 5. Plot of birefringence and EML *versus* core porosity at 1 THz ($\Lambda = 200$ μm, $t = 0.015\Lambda$).

For Kagome-structured PCFs that may be fabricated by the stack-and-drawing, extrusion and even the flexible and accurate 3D printing technique, the relative strut-thickness (t/Λ) is also an important parameter that can affect propagation properties of the fiber.[22–25] Figure 6 shows the variation of birefringence and EML with t/Λ for the designed THz fiber. It can be seen that birefringence decreases, the EML of y-polarized fundamental mode increases and the EML of x-polarized fundamental mode has little change with the increase of relative strut-thickness. Therefore, the relative strut-thickness should be as small as possible in order to achieve a high birefringence and a low EML. So a small relative strut-thickness $t/\Lambda = 1.5\%$ that has been experimentally reported[22] is adopted for the designed fiber.

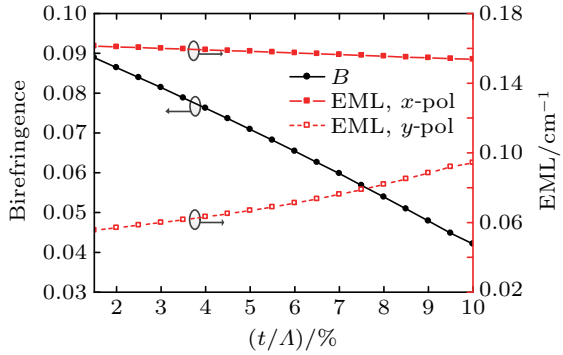


Fig. 6. Plot of birefringence and EML *versus* relative strut thickness at 1 THz ($\Lambda = 200$ μm, core porosity = 55%).

By comparing Figs. 3–6, the conclusions are obtained as follows.

(i) The structural parameter dependence of birefringence and loss are different and even conflicting with each other as a result of their different origins.

(ii) Birefringences are of the same order of magnitude (10^{-2}) although their variations with structural parameters (lattice pitch, cladding hole ring number, core porosity and relative strut thickness) are different. However, the variations of EML with structural parameters are relatively dramatic (from 0.04 cm^{-1} to 0.25 cm^{-1}). So the structural parameters with lower loss are adopted rather than the ones with higher birefringence when they are conflicting with each other (as shown in Fig. 5).

(iii) Considering a tradeoff between high birefringence and low EML, the structural parameters with $\Lambda = 200$ μm, rings = 2, core porosity = 55% and $t/\Lambda = 1.5\%$ are adopted for the optimal THz PCF.

The V-parameter and dispersion characteristics of the designed optimum THz PCF are shown in Figs. 7(a) and 7(b), respectively. It is observed that the y polarization operates in single mode condition over the whole operating frequency spectrum, while the x polarization operates in single mode condition when the frequency is less than 1.17 THz. It can be seen that both the x- and y-polarized fundamental modes have low and flat dispersion within its single mode operating frequency spectrum. Especially the dispersion value of y-polarized fundamental mode is 0 ± 0.45 ps $\cdot$ THz^{-1} $\cdot$ cm^{-1} over a wide frequency range (0.5 THz–1.5 THz), which can be regarded as an ultra-flattened and near-zero dispersion.

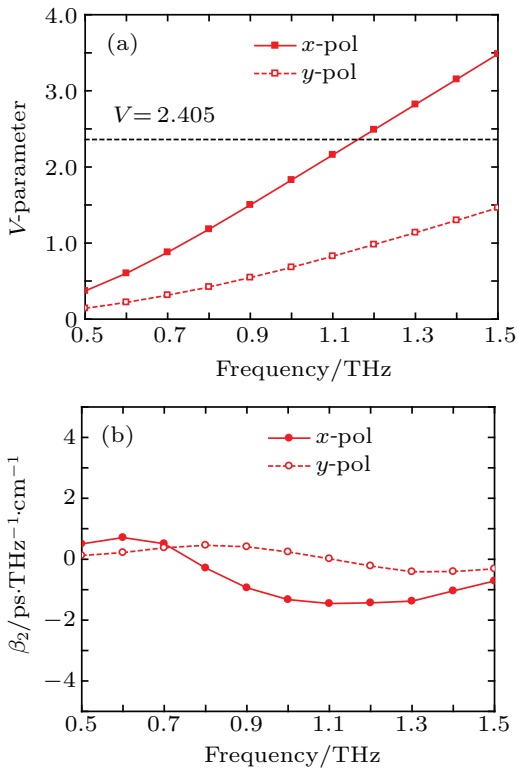


Fig. 7. (a) V-parameter and (b) dispersion *versus* frequency of the fundamental modes for the optimized THz PCF.

The propagation properties of the designed THz PCF are compared with the recently reported PCF's as listed in Table 1. It can be seen that the designed THz PCF shows improved propagation properties, *i.e.*, higher birefringence, lower EML, ultra-flattened, and near-zero dispersion over a wider frequency range individually or wholly than the ever reported THz PCFs.

Table 1. Comparison of propagation properties between designed THz PCF and other PCF's.

Reference	Bulk material	B	EML/cm^{-1}	β_2/ps·THz^{-1}·cm^{-1}
[13]	Topas	0.047 (at 1.22 THz)	0.035 (at 1.22 THz)	–
[14]	Topas	0.0483 (at 1 THz)	0.085 (at 1 THz)	±0.51 (at 1.2–1.8 THz)
[16]	Topas	0.018 (at 1 THz)	0.07 (at 1 THz)	1.1 ± 0.02 (at 0.8–1.2 THz)
[17]	Zeonex	0.079 (at 1 THz)	0.05 (at 1 THz)	0.49 ± 0.05 (at 0.9–1.7 THz)
[26]	Topas	0.078 (at 0.95 THz)	0.09 (at 0.95 THz)	< 0.5 (at 0.75–0.95 THz)
[27]	Topas	0.0119 (at 1 THz)	0.0689 (at 1 THz)	–
This paper	Topas	0.089 (at 1 THz)	0.055 (at 1 THz)	0 ± 0.45 (at 0.5–1.5 THz)

It is necessary to discuss the fabrication possibilities of our proposed THz PCF for its practical implementation. There are many ways to fabricate the polymer-based PCFs compared with silica-based ones. Beside the stacking-and-drawing of capillaries, which is suitable for making PCFs with circular air holes arranged in triangular lattice, the extrusion, casting, molding, and drilling have been used successfully to made polymer PCFs with various complex and asymmetrical structures.[28] Moreover, the most recently developed 3D printing technique has been used to produced THz waveguides with complicated and small features, and the most advanced laser-based 3D printing techniques can realize a printing resolution of the order of micrometer in x and y dimensions.[29,30] Kagome lattice PCF and porous core PCF with non-circular slot air holes are fabricated successfully by using the stack-and-draw, 3D printing, extrusion techniques, *etc*.[23,31,32]

The structure of our proposed THz PCF with Kagome lattice cladding and slot air holes is relatively simple and robust compared with the PCFs operating in the telecommunication range, and the fabrication possibility is considered during the structural parameter optimization. So, it is possible to fabricate the designed THz PCF by using or combining the existing techniques, such as drawing from a 3D-printed preform.[33] In our previous papers, experimental investigations have been carried out for the fabrication of polymer-based PCFs.[34,35] The designed THz PCF in this paper will be fabricated in our consequent researches.

4. Conclusions

An improved Kagome PCF with slot air holes in a rectangular core is designed for the transmission of THz waves. Structural parameter dependence of the propagation properties such as birefringence, material absorption loss (effective modal loss), confinement loss and dispersion are numerically investigated by using the full-vector FEM. The simulation results indicate that even two rings of cladding holes can obtain a negligible confinement loss. Ultra high birefringence of 0.089 and low effective material absorption loss of 0.055 cm^{-1} are obtained at 1 THz for the optimized fiber structure. Besides, the y-polarized fundamental mode shows an ultra-flattened and near-zero dispersion of 0 ± 0.45 ps·THz^{-1}·cm^{-1} over 0.5 THz–1.5 THz. The designed THz PCF shows improved propagation properties compared with the recent reported PCF's and its structure is relatively simple and manufacturable. Thus, the designed Kagome PCF has potential applications in fields of THz communication and polarization maintaining systems.

References

[1] Yu Y Y, Li X Y, He K P and Sun B 2016 *Chin. Phys. B* **25** 028703
[2] Wang Y, Ren Y, Chen L, Song C, Li C, Zhang C, Xu D and Yao J 2018 *Chin. Phys. B* **27** 114204
[3] Withayachumnankul W, Fischer B M, Lin H and Abbott D 2008 *J. Opt. Soc. Am. B* **25** 1059
[4] Strachan C J, Taday P F, Newnham D A, Gordon K C, Zeitler J A, Pepper M and Rades T 2005 *J. Pharm. Sci.* **94** 837
[5] Wang M, Wang J F, Wu Q Y and Huang Y X 2014 *Acta Phys. Sin.* **63** 154101 (in Chinese)
[6] Wang K and Mittleman D M 2004 *Nature* **432** 376
[7] Bowden B, Harrington J A and Mitrofanov O 2007 *Opt. Lett.* **32** 2945
[8] Skorobogatiy M and Dupuis A 2007 *Appl. Phys. Lett.* **90** 113514
[9] Mendis R and Grischkowsky D 2000 *J. Appl. Phys.* **88** 4449
[10] Wang J L, Yao J Q, Chen H M, Bing P B, Li Z Y and Zhong K 2011 *Acta Phys. Sin.* **60** 104219 (in Chinese)
[11] Cho M, Kim J, Park H, Han Y, Moon K, Jung E and Han H 2008 *Opt. Express* **16** 7
[12] Atakaramians S, Shahraam A V, Fischer B M, Abbott D and Monro T M 2009 *Opt. Commun.* **282** 36
[13] Chen N, Liang J and Ren L 2013 *Appl. Opt.* **52** 5297
[14] Hasan M R, Anower M S, Islam M A and Razzak S M A 2016 *Appl. Opt.* **55** 4145
[15] Wu Z, Shi Z, Xia H, Zhou X, Deng Q, Huang J, Jiang X and Wu W 2016 *IEEE Photon. J.* **8** 4502711
[16] Habib M A, Anower M S and Hasan M R 2018 *Opt. Commun.* **423** 140
[17] Islam M S, Sultana J, Dinovitser A, Ng W H and Abbott D 2018 *Opt. Commun.* **413** 242
[18] Nielsen K, Rasmussen H K, Adam A J, Planken P C, Bang O and Jepsen P U 2009 *Opt. Express* **17** 8592
[19] Khanarian G 2001 *Opt. Eng.* **40** 1024
[20] Ung B, Mazhorova A, Dupuis A, Rozé M and Skorobogatiy M 2011 *Opt. Express* **19** B848
[21] Liang J, Ren L, Chen N and Zhou C 2013 *Opt. Commun.* **295** 257
[22] Argyros A and Pla J 2007 *Opt. Express* **15** 7713
[23] Couny F, Benabid F and Light P S 2006 *Opt. Lett.* **31** 3574
[24] Wang Y Y, Wheeler N V, Couny F, Roberts P J and Benabid F 2011 *Opt. Lett.* **36** 669
[25] Anthony J, Leonhardt R, Leonsaval S and Argyros A 2011 *Opt. Express* **19** 18470
[26] Luo J, Chen S, Qu H, Su Z, Li L and Tian F 2018 *J. Lightwave Technol.* **36** 3242
[27] Kawsar A, Sawrab C, Kumar P B, Md S I, Shuvo S, Md I I and Sayed A 2017 *Appl. Opt.* **56** 3477
[28] Large M C J, Ponrathnam S, Argyros A, Bassett I M, Punjari N S, Cox F, Lwin R, Barton G W and Van E M A 2006 *Mol. Cryst. Liq. Cryst.* **446** 219
[29] Van P L D, Gorecki J, Numkam F E, Apostolopoulos V and Poletti F 2018 *Appl. Opt.* **57** 3953
[30] Li J, Nallappan K, Guerboukha H and Skorobogatiy M 2017 *Opt. Express* **25** 4126
[31] Yang J, Zhao J, Gong C, Tian H, Sun L, Chen P, Lin L and Liu W 2016 *Opt. Express* **24** 22454
[32] Atakaramians S, Afshar V S, Ebendorff-Heidepriem H, Nagel M, Fischer B M, Abbott D and Monro T M 2009 *Opt. Express* **17** 14053
[33] Cook K, Canning J, Leon-Saval S, Reid Z, Hossain M A, Comatti J, Luo Y and Peng G 2015 *Opt. Lett.* **40** 3966
[34] Kong D P and Wang L L 2009 *Opt. Lett.* **34** 2435
[35] Chen Q, Kong D P, Miao J, He X Y, Zhang J and Wang L L 2017 *Acta Phot. Sin.* **46** 0406001 (in Chinese)